Applied Mathematics & Information Sciences
An International Journal

http://dx.doi.org/10.18576/amis/160104

Melting Heat Transfer Effects on Flow of a Micropolar Fluid with Heat Generation(Absorption) in Slip Flow Regime

Shimaa E. Waheed and Ahmed M. Megahed*

Department of Mathematics, Faculty of Science, Benha University, Egypt

Received: 2 Jul. 2021, Revised: 2 Sep. 2021, Accepted: 27 Oct. 2021
Published online: 1 Jan. 2022

Abstract: In this paper, the heat transfer mechanism to the non-Newtonian micropolar slip fluid flow over a stretching sheet in the presence of the melting heat transfer with heat generation(absorption) have been studied. With appropriate dimensionless transformations, the boundary layer equations governing the physical problem are reduced to a system of non-linear ordinary differential equations valid in the melting regime. Solutions of the system are obtained by employing the Chebyshev spectral method. Numerical solutions are obtained for different values of the material parameter, slip parameter, heat generation(absorption) parameter, local Eckret number, melting parameter, microrotation parameter and thermal conductivity parameter. From this solutions we find that, the velocity increases with the increase of the material parameter, local Eckret number and melting parameter the opposite is true as slip parameter and heat generation(absorption) parameter. Also, the angular velocity increases with the increase of heat generation(absorption) parameter and microrotation parameter, while it decreases as the material parameter, slip parameter and local Eckret number. The temperature increases as the material parameter increases but it decreases as slip parameter, heat generation(absorption) parameter, local Eckret number, melting parameter and thermal conductivity parameter. Finally, the values of the surface shear stress, the wall couple stress and the local Nusselt number are introduced tabularly.

Keywords: Melting effect; Micropolar fluid; Heat generation (absorption), Slip velocity, Variable thermal conductivity.

Nomenclature

B_0	strength of a uniform magnetic field
c_p	specific heat at constant pressure
c_s	heat capacity of the solid surface
C_{f_x}	local skin-friction coefficient
E_c	local Eckret number
M^*	magnetic parameter
f	dimensionless velocity
G	micro-rotation parameter
G_1	micro-rotation constant
h	dimensionless microrotation
k	gyro-viscosity
K	material parameter
k_1	permeability
M	melting parameter
M_x	dimensionless wall couple stress
m_0	boundary parameter
m_w	wall couple stress
N	dimensional component of microrotation vector normal to the $X-Y$ plane
N_{u_x}	local Nusselt number
Pr	Prandtl number
Q_0	heat generation or absorption constant
q_w	heat transfer from the plate
Re_x	local Reynolds number.
T	fluid temperature
T_0	solid temperature
T_m	temperature of the melting surface
T_∞	free stream condition
u, v	dimensional components of velocities along and perpendicular to the plate, respectively
x, y	dimensional distances along and perpendicular to the plate, respectively

* Corresponding author e-mail: shimaa_ezat@yahoo.com

© 2022 NSP
Natural Sciences Publishing Cor.

Greek symbols

α	slip parameter
γ	heat generation or absorption parameter
θ	dimensionless temperature
κ_∞	thermal conductivity of the ambient fluid
λ	latent heat fluid
λ^*	the slip coefficient
μ	dynamic viscosity
ρ	fluid density
τ_w	surface shear stress
σ	electrical conductivity,
ε	thermal conductivity parameter

Superscripts

$\prime$	differentiation with respect to η

1 Introduction

In 1964, The basis of the theory of a novel class of non-Newtonian fluids which called as a continuum theory of microfluids have been given by Eringen [1]. This class of fluids takes into accounts the local motions and deformations of the primitive elements of fluids. According to the assumptions of this theory, microfluids sometimes known as the micromorphic or microstructure theory. On the other hand, he proved that the micropolar fluids are special case of microfluids. Also, he defined this type of fluid as the fluids which contain molecular constituents whose size is not negligible when compared with the geometrical characteristic length. Eringen [2] expanded the micropolar fluids theory which takes into account the local motions and deformations of the primitive elements of fluids by taking into consideration the influence of microrotation of these constituents. This theory may be used to provide an explanation for the flow of polymeric fluids, colloidal fluids, liquid crystals, animal blood and the equations governing the flow of micropolar fluid involve the microrotation vector and the gyration parameter in addition to the classical velocity vector field. After that, Eringen [3] has generalized the micropolar fluid theory to take into consideration the thermal impacts, which is scientifically called the theory of thermomicrofluids. Based on the pioneering work of [3], many studies have been carried out in the past to analyze the characteristics of the boundary layer flow of a non-Newtonian micropolar fluid under various boundary conditions [4-6]. Another advantage for the micropolar fluids is that it can be more suitable in modeling the body fluids and the cerebro-spinal fluid. Powel [7] has shown that the fluid flowing in the brain can be modeled mathematically as a non-Newtonian micropolar fluid. The number of published papers in the field of micropolar fluid presently exceeds several hundred papers. As instance, Takhar et al. [8] analyzed the viscous dissipation in a steady, incompressible micropolar boundary layer flow over a stretching sheet. Bhargava et al. [9] derived a similarity solution for the mixed convection flow of a continuously moving flat plate placed in a parallel moving stream of a micropolar fluid. So far, there have been many studies focusing on the non-Newtonian models especially; the micropolar fluids model [10-13]. It is known that MHD flows have received considerable attention because of their practical applications in power generation, geophysics and astrophysics [14]. On the other hand the significance of slip velocity phenomenon for the boundary layer thickness control in the field of aerodynamics and space science is well recognized [15].

The technological and engineering applications of the flow of non-Newtonian thermo micro-polar fluids was the motivation for a an immense number of recent work. So, some of recent researches regarding this important topic under different physical situation such as melting phenomenon [16], chemical reaction effect [17] and Soret and Dufour impact [18] are discussed. Hence it is of interest to make an investigation in order to analyze the influence of the viscous dissipation, the heat generation and the slip velocity on the characteristics of an electrically conducting non-Newtonian micropolar fluid flow with melting phenomenon. Numerical solutions of the proposed problem are obtained by using the Chebyshev spectral method for the variable thermal conductivity that is proportional linearly to the temperature. The results are presented for a range of values of all material parameters of the fluid.

2 Formulation of the problem

We are consider the flow of an incompressible micropolar fluid towards a horizontal plate. It is assumed that the plate constitutes the interface between the liquid phase and the solid phase during melting inside the porous matrix at the steady state. The $x-$axis being along the plate and the $y-$ axis normal to it respectively. The plate is at constant temperature T_m at which the material of the porous matrix melts. The liquid phase temperature $T_\infty(> T_m)$ and the temperature of the solid far from the interface in $T_0(< T_m)$. The flow is steady, Laminar and two-dimensional. Under the usual boundary-layer and the Boussinesq approximations , the governing equations taking in the presence of heat generation(absorption) at the energy equation for a micropolar fluid, which can be written as:

$$\frac{\partial u}{\partial x}+\frac{\partial v}{\partial y}=0, \tag{1}$$

$$u\frac{\partial u}{\partial x}+v\frac{\partial u}{\partial y}=(\frac{\mu+k}{\rho})\frac{\partial^2 u}{\partial y^2}+\frac{k}{\rho}\frac{\partial N}{\partial y}-\frac{\sigma B_0^2}{\rho}u, \tag{2}$$

$$G_1\frac{\partial^2 N}{\partial y^2}-(2N+\frac{\partial u}{\partial y})=0, \tag{3}$$

$$u\frac{\partial T}{\partial x}+v\frac{\partial T}{\partial y}=\frac{1}{\rho c_p}\frac{\partial}{\partial y}(\kappa\frac{\partial T}{\partial y})+\frac{Q_0}{\rho c_p}(T-T_\infty)$$

© 2022 NSP
Natural Sciences Publishing Cor.

$$+\frac{1}{\rho c_p}\frac{\partial u}{\partial y}[(\mu+k)\frac{\partial u}{\partial y}+kN], \tag{4}$$

where u and v are the velocity components in the x and y directions; respectively. N is the component of the micro-rotation vector normal to the $x-y$ plane, T is the fluid temperature, μ is the dynamic viscosity, k is the gyro-viscosity (or vortex viscosity), ρ is the fluid density, σ is the electrical conductivity,B_0 is the strength of a uniform magnetic field, $G_1 = \frac{\gamma^*}{k}$ is the microrotation constant, $\kappa = \kappa_\infty(1+\varepsilon\theta)$ is the variable thermal conductivity of the fluid, ε thermal conductivity parameter, c_p is the specific heat at constant pressure and Q_0 is the heat generation or absorption constant.

We assume that the boundary conditions are the following:

$$u = ax+\lambda^*[(\mu+k)\frac{\partial u}{\partial y}+kN], \quad N=-m_0\frac{\partial u}{\partial y}, \quad T = T_m, \quad at \quad y=0, \tag{5}$$

$$u\to 0, \quad N\to 0, \quad T\to T_\infty, \quad as \quad y\to\infty$$

and

$$\kappa(\frac{\partial T}{\partial y})_{y=0} = \rho[\lambda + c_s(T_m - T_0)]v(x,0), \tag{6}$$

where m_0 $(0\le m_0\le 1)$ is the boundary parameter.If $m_0=0$, we obtain $N=0$ which is the no-spin condition i.e. the microelements in a concentrated particle flow close to the wall are not able to rotate (as stipulated by Jena and Mathur [19]). The case $m_0 = 1/2$, represents the weak concentration of microelements. The case corresponding to $m_0 = 1$ is used for the modelling of turbulent boundary layer flow (see Peddison and Mc Nitt [20]), λ^* is the slip coefficient, λ is the latent heat fluid and c_s is the heat capacity of the solid surface. Eq.(6) states that the heat conducted to the melting surface is equal to the heat of melting plus the sensible heat required to raise the solid temperature T_0 to its melting temperature T_m (see Epstein and Cho [21] and Bachok et al. [22]).

We introduce the following dimensionless variables :

$$\eta = (\frac{a}{\nu})^{1/2}y, \quad N = ax(\frac{a}{\nu})^{1/2}h(\eta),$$

$$u = axf'(\eta), \quad v = -(a\nu)^{1/2}f, \quad \theta(\eta) = \frac{T-T_m}{T_\infty - T_m}. \tag{7}$$

Through Eq. (7), the continuity equation (1) is automatically satisfied and Eqs. (2)-(4) will give then:

$$(1+K)f''' + ff'' - f'^2 + Kh' - M^*f' = 0, \tag{8}$$

$$Gh'' - (2h+f'') = 0, \tag{9}$$

$$\frac{1}{Pr}(1+\varepsilon\theta)\theta'' + \frac{1}{Pr}\varepsilon\theta'^2 + f\theta'$$

$$+\gamma(\theta-1) + E_c[(1+K)f''^2 + Khf''] = 0. \tag{10}$$

The transformed boundary conditions are then given by:

$$f' = 1+\alpha[(1+K)f''+Kh], \quad Prf + M(1+\varepsilon\theta)\theta' = 0,$$

$$h = -m_0 f'', \quad \theta = 0, \quad at \quad \eta = 0, \tag{11}$$

$$f'\to 0, \quad h\to 0, \quad \theta\to 1, \quad as \quad \eta\to\infty,$$

where primes denote differentiation with respect to η, $K = \frac{k}{\mu}$ is the material parameter, $M^* = \frac{\sigma B_0^2}{\rho c_p}$ is the magnetic parameter, $\alpha = \lambda^*\rho(a\nu)^{1/2}$ is the slip parameter, $E_c = \frac{u_w^2}{c_p(T_\infty - T_m)}$ is the local Eckret number, $G = G_1 a/\nu$ is the microrotation parameter, $Pr = \mu c_p/\kappa_\infty$ is the Prandtl number, $\gamma = \frac{Q_0}{a\rho c_p}$ is the heat generation $(\gamma>0)$ or absorption $(\gamma<0)$ parameter and M is the dimensionless melting parameter which is defined as

$$M = \frac{c_p(T_\infty - T_m)}{\lambda + c_s(T_m - T_0)}. \tag{12}$$

The melting parameter is a combination of the two Stefan numbers $c_f(T_\infty - T_m)/\lambda$ and $c_s(T_m - T_0)/\lambda$ for the liquid and solid phases, respectively.

The physical quantities of interest are the local skin-friction coefficient C_{f_x}, the dimensionless wall couple stress M_x and the local Nusselt number N_{u_x}, which are defined respectively; as:

$$C_{f_x} = \frac{-2\tau_w}{\rho(u_w)^2}, \quad M_x = \frac{m_w}{\rho a\nu u_w x^2}, \quad Nu_x = \frac{xq_w}{\kappa(T_\infty - T_m)}, \tag{13}$$

where the surface shear stress τ_w, the wall couple stress m_w and the heat transfer from the plate q_w are defined by:

$$\tau_w = [(\mu+K)\frac{\partial u}{\partial y} + KN]_{y=0}, \quad m_w = \gamma^*(\frac{\partial N}{\partial y})_{y=0}$$

$$, \quad q_w = -[\kappa\frac{\partial T}{\partial y}]_{y=0}. \tag{14}$$

Using the similarity variables (13), we get:

$$\frac{1}{2}C_{f_x}Re_x^{1/2} = (1+K(1-m_0))f''(0),$$

$$M_x Re_x = KGh'(0), \quad Nu_x Re_x^{-1/2} = -\theta'(0), \tag{15}$$

where $R_{e_x} = (\frac{u_w x}{\nu})$ is the local Reynolds number.

© 2022 NSP
Natural Sciences Publishing Cor.

3 Method of solution

The system of boundary layer equations (8)-(11) have the domain $0 \leq \eta \leq \eta_\infty$, where η_∞ is one end of the user specified computational domain. Using the algebraic mapping:

$$\chi = 2\frac{\eta}{\eta_\infty} - 1,$$

the unbounded region $[0,\infty)$ is mapped into the finite domain $[1,-1]$, and we can transform the problem expressed by equations (8)-(11) to the system:

$$(1+K)f'''(\chi) + (\tfrac{\eta_\infty}{2})(f(\chi)f''(\chi) - f'^2(\chi))$$

$$+(\frac{\eta_\infty}{2})^2[Kh'(\chi) - M^* f'(\chi)] = 0, \qquad (16)$$

$$Gh''(\chi) - (2(\frac{\eta_\infty}{2})^2 h(\chi) + f''(\chi)) = 0, \qquad (17)$$

$$\tfrac{1}{Pr}(1+\varepsilon\theta(\chi))\theta''(\chi) + \tfrac{1}{Pr}\varepsilon\theta'^2(\chi) + (\tfrac{\eta_\infty}{2})f(\chi)\theta'(\chi) + (\tfrac{\eta_\infty}{2})^2\gamma(\theta(\chi)-1)$$

$$+E_c((1+K)(\frac{2}{\eta_\infty})^2 f''^2(\chi) + Kh(\chi)f''(\chi)) = 0. \qquad (18)$$

The transformed boundary conditions are given by:

$$Prf(-1) + M(1+\varepsilon\theta(-1))(\tfrac{2}{\eta_\infty})\theta'(-1) = 0, \quad f'(-1) = (\tfrac{\eta_\infty}{2}) + \alpha(1+K(1-m_0))(\tfrac{2}{\eta_\infty})f''(-1), \quad f'(1) = 0$$

$$h(-1) = -m_0(\frac{2}{\eta_\infty})^2 f''(-1), \quad h(1) = 0 \qquad (19)$$

$$\theta(-1) = 0, \quad \theta(1) = 1,$$

Our technique is accomplished by starting with a Chebyshev approximation for the highest order derivatives, f''', h'' and θ'' and generating approximations to the lower order derivatives f'', f', f, h', h, θ' and θ as follows:

Setting $f''' = \phi(\chi)$, $h'' = \psi(\chi)$ and $\theta'' = \zeta(\chi)$, then by integration we obtain:

$$f''(\chi) = \int_{-1}^{\chi} \phi(\chi)d\chi + C_1^f. \qquad (20)$$

$$f'(\chi) = \int_{-1}^{\chi}\int_{-1}^{\chi} \phi(\chi)d\chi d\chi + C_1^f(\chi+1) + C_2^f. \qquad (21)$$

$$f(\chi) = \textstyle\int_{-1}^{\chi}\int_{-1}^{\chi}\int_{-1}^{\chi} \phi(\chi)d\chi d\chi d\chi$$

$$+C_1^f\frac{(\chi+1)^2}{2} + C_2^f(\chi+1) + C_3^f. \qquad (22)$$

$$h'(\chi) = \int_{-1}^{\chi} \psi(\chi)d\chi + C_1^h. \qquad (23)$$

$$h(\chi) = \int_{-1}^{\chi}\int_{-1}^{\chi} \psi(\chi)d\chi d\chi + C_1^h(\chi+1) + C_2^h. \qquad (24)$$

$$\theta'(\chi) = \int_{-1}^{\chi} \zeta(\chi)d\chi + C_1^\theta. \qquad (25)$$

$$\theta(\chi) = \int_{-1}^{\chi}\int_{-1}^{\chi} \zeta(\chi)d\chi d\chi + C_1^\theta(\chi+1) + C_2^\theta. \qquad (26)$$

We obtain, from the boundary condition (19):

$$C_1^f = \tfrac{-1}{2+\alpha(1+K(1-m_0))(\frac{2}{\eta_\infty})}(\tfrac{\eta_\infty}{2}) - \tfrac{1}{2+\alpha(1+K(1-m_0))(\frac{2}{\eta_\infty})}\textstyle\int_{-1}^{1}\int_{-1}^{\chi}\phi(\chi)d\chi d\chi,$$

$$C_2^f = (\tfrac{\eta_\infty}{2}) + \alpha(1+K(1-m_0))(\tfrac{2}{\eta_\infty})C_1^f,$$

$$C_3^f = \tfrac{M}{2Pr}(\tfrac{2}{\eta_\infty})\textstyle\int_{-1}^{1}\int_{-1}^{\chi}\zeta(\chi)d\chi d\chi - \tfrac{M}{2Pr}(\tfrac{2}{\eta_\infty}),$$

$$C_1^h = -\tfrac{1}{2}\textstyle\int_{-1}^{1}\int_{-1}^{\chi}\psi(\chi)d\chi - \tfrac{1}{2}C_2^h,$$

$$C_2^h = \tfrac{m_0}{2+\alpha(1+K(1-m_0))(\frac{2}{\eta_\infty})}(\tfrac{2}{\eta_\infty})^2\textstyle\int_{-1}^{1}\int_{-1}^{\chi}\phi(\chi)d\chi d\chi + \tfrac{m_0}{2+\alpha(1+K(1-m_0))(\frac{2}{\eta_\infty})}(\tfrac{2}{\eta_\infty}),$$

$$C_1^\theta = \tfrac{1}{2} - \tfrac{1}{2}\textstyle\int_{-1}^{1}\int_{-1}^{\chi}\zeta(\chi)d\chi d\chi,$$

$$C_2^\theta = 0.$$

We can give approximations to equations (20)-(26) as follows:

$$f_i(\chi) = \textstyle\sum_{j=0}^{n} l_{ij}^f\phi_j + d_i^f, \quad f_i'(\chi) = \sum_{j=0}^{n} l_{ij}^{f1}\phi_j +$$

$$d_i^{f1}, \quad f_i''(\chi) = \sum_{j=0}^{n} l_{ij}^{f2}\phi_j + d_i^{f2}. \qquad (27)$$

$$h_i(\chi) = \textstyle\sum_{j=0}^{n} l_{ij}^\theta\psi_j + \sum_{j=0}^{n} l_{ij}^h\phi_j + d_i^h, \quad h_i'(\chi) = \sum_{j=0}^{n} l_{ij}^{\theta 1}\psi_j$$

$$+\sum_{j=0}^{n} l_{ij}^{h1}\phi_j + d_i^{h1}, \qquad (28)$$

$$\theta_i(\chi) = \sum_{j=0}^{n} l_{ij}^\theta\zeta_j + d_i^\theta, \quad \theta_i'(\chi) = \sum_{j=0}^{n} l_{ij}^{\theta 1}\zeta_j + d_i^{\theta 1}, \qquad (29)$$

for all $i = 0(1)n$, where

$$l_{ij}^\theta = b_{ij}^2 - \tfrac{(\chi_i+1)}{2}b_{nj}^2, \quad d_i^\theta = \tfrac{(\chi_i+1)}{2},$$

$$l_{ij}^{\theta 1} = b_{ij} - \tfrac{1}{2}b_{nj}^2, \quad d_i^{\theta 1} = \tfrac{1}{2},$$

$$l_{ij}^h = \tfrac{m_0}{2+\alpha(1+K(1-m_0))(\frac{2}{\eta_\infty})}(\tfrac{2}{\eta_\infty})^2(1 - \tfrac{(\chi_i+1)}{2})b_{nj}^2, \quad d_i^h = -\tfrac{m_0}{2+\alpha(1+K(1-m_0))(\frac{2}{\eta_\infty})}(\tfrac{2}{\eta_\infty})[\tfrac{(\chi_i+1)}{2} - 1],$$

$$l_{ij}^{h1} = -\tfrac{m_0}{2(2+\alpha(1+K(1-m_0))(\frac{2}{\eta_\infty}))}(\tfrac{2}{\eta_\infty})^2 b_{nj}^2, \quad d_i^{h1} = -\tfrac{m_0}{2(2+\alpha(1+K(1-m_0))(\frac{2}{\eta_\infty}))}(\tfrac{2}{\eta_\infty}),$$

© 2022 NSP
Natural Sciences Publishing Cor.

$$l_{ij}^{f}=b_{ij}^{3}-(\frac{(\chi_i+1)^2}{2(2+\alpha(1+K(1-m_0))(\frac{2}{\eta_\infty}))}+\frac{\alpha(1+K(1-m_0))(\frac{2}{\eta_\infty})(\chi_i+1)}{2+\alpha(1+K(1-m_0))(\frac{2}{\eta_\infty})})b_{nj}^{2},\quad l_{ij}^{\bar{f}}=\frac{M}{2Pr}(\frac{2}{\eta_\infty})b_{nj}^{2},$$

$$d_i^{f}=-(\frac{(\chi_i+1)^2}{2(2+\alpha(1+K(1-m_0))(\frac{2}{\eta_\infty}))}+\frac{2+\alpha(1+K(1-m_0))(\frac{2}{\eta_\infty})(\chi_i+1)}{2+\alpha(1+K(1-m_0))(\frac{2}{\eta_\infty})}-(\chi_i+1))(\frac{\eta_\infty}{2})-\frac{M}{2Pr}(\frac{2}{\eta_\infty}),$$

$$l_{ij}^{f1}=b_{ij}^{2}-(\frac{(\chi_i+1)}{2+\alpha(1+K(1-m_0))(\frac{2}{\eta_\infty})}+\frac{\alpha(1+K(1-m_0))(\frac{2}{\eta_\infty})}{2+\alpha(1+K(1-m_0))(\frac{2}{\eta_\infty})})b_{nj}^{2},\quad l_{ij}^{\bar{f}1}=0,$$

$$d_i^{f1}=-(\frac{(\chi_i+1)}{2+\alpha(1+K(1-m_0))(\frac{2}{\eta_\infty})}+\frac{\alpha(1+K(1-m_0))(\frac{2}{\eta_\infty})}{2+\alpha(1+K(1-m_0))(\frac{2}{\eta_\infty})}-1)(\frac{\eta_\infty}{2}),$$

$$l_{ij}^{f2}=b_{ij}-\frac{1}{2+\alpha(1+K(1-m_0))(\frac{2}{\eta_\infty})}b_{nj}^{2},\quad l_{ij}^{\bar{f}2}=0,\quad d_i^{f2}=\frac{-1}{2+\alpha(1+K(1-m_0))(\frac{2}{\eta_\infty})}(\frac{\eta_\infty}{2}),$$

where $\chi_i=-cos(\frac{i\pi}{n})$ are the Chebyshev points.

$$b_{ij}^{2}=(\chi_i-\chi_j)b_{ij},$$

and b_{ij} are the elements of the matrix B, which are given in Ref. [23].

One can transform the system of equations (16)-(18) to the following system of nonlinear equations in the highest derivatives by using equations (27)-(29), into the following Chebyshev spectral equations:

$$(1+K)\phi_i+(\frac{\eta_\infty}{2})[(\sum_{j=0}^{n}l_{ij}^{f}\phi_j+\sum_{j=0}^{n}l_{ij}^{\bar{f}}\zeta_j+d_i^{f})(\sum_{j=0}^{n}l_{ij}^{f2}\phi_j+\sum_{j=0}^{n}l_{ij}^{\bar{f}2}\zeta_j+d_i^{f2})-(\sum_{j=0}^{n}l_{ij}^{f1}\phi_j+\sum_{j=0}^{n}l_{ij}^{\bar{f}1}\zeta_j+d_i^{f1})^2]+(\frac{\eta_\infty}{2})^2[K(\sum_{j=0}^{n}l_{ij}^{\theta1}\psi_j+\sum_{j=0}^{n}l_{ij}^{h1}\phi_j+d_i^{h1})-M^{*}(\sum_{j=0}^{n}l_{ij}^{f1}\phi_j+\sum_{j=0}^{n}l_{ij}^{\bar{f}1}\zeta_j+d_i^{f1}))]=0, \tag{30}$$

$$G\psi_i-(2(\frac{\eta_\infty}{2})^2(\sum_{j=0}^{n}l_{ij}^{\theta}\psi_j+\sum_{j=0}^{n}l_{ij}^{h}\phi_j+d_i^{h})+(\sum_{j=0}^{n}l_{ij}^{f2}\phi_j+\sum_{j=0}^{n}l_{ij}^{\bar{f}2}\zeta_j+d_i^{f2}))=0, \tag{31}$$

$$\frac{1}{Pr}(1+\varepsilon(\sum_{j=0}^{n}l_{ij}^{\theta}\zeta_j+d_i^{\theta}))\zeta_i+\frac{1}{Pr}\varepsilon(\sum_{j=0}^{n}l_{ij}^{\theta}\zeta_j+d_i^{\theta})^2+(\frac{\eta_\infty}{2})(\sum_{j=0}^{n}l_{ij}^{f}\phi_j+\sum_{j=0}^{n}l_{ij}^{\bar{f}}\zeta_j+d_i^{f})(\sum_{j=0}^{n}l_{ij}^{\theta1}\zeta_j+d_i^{\theta1})+(\frac{\eta_\infty}{2})^2\gamma(\varepsilon(\sum_{j=0}^{n}l_{ij}^{\theta}\zeta_j+d_i^{\theta})-1)+E_c[(1+K)(\frac{2}{\eta_\infty})^2(\sum_{j=0}^{n}l_{ij}^{f2}\phi_j+\sum_{j=0}^{n}l_{ij}^{\bar{f}2}\zeta_j+d_i^{f2})^2+K(\sum_{j=0}^{n}l_{ij}^{f2}\phi_j+\sum_{j=0}^{n}l_{ij}^{\bar{f}2}\zeta_j+d_i^{f2})(\sum_{j=0}^{n}l_{ij}^{\theta}\psi_j+\sum_{j=0}^{n}l_{ij}^{h}\phi_j+d_i^{h})]=0. \tag{32}$$

This system is then solved using Newton's iteration method with $n=12$, the computer program was executed in mathematica 4 running on a PC.

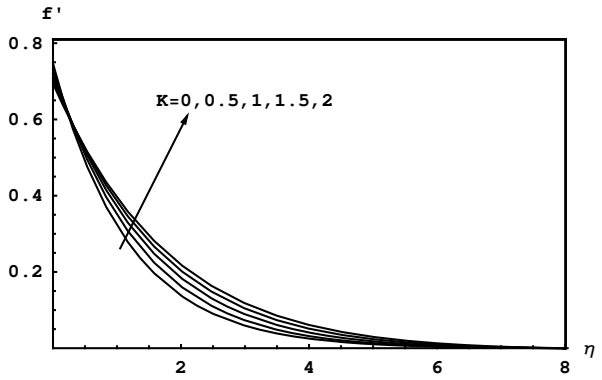

Fig. 1: Velocity profiles $f'(\eta)$ for different values of K with $\varepsilon=0.2, M^{*}=0.1, \alpha=0.1, G=2.0, E_c=0.5, M=2.0, P_r=1.0, m_0=0.5$ and $\gamma=0.2$

4 Results and discussion

The investigations of the effect of melting phenomenon and the slip velocity on the non-Newtonian micropolar fluid flow and heat transfer along a horizontal stretching sheet which exposed to a magnetic field carried out in the preceding sections enable us to come in with the following results. So, we can show the effects of the various governing parameters such as the material parameter, the slip parameter, the heat generation (absorption) parameter, the local Eckret number, the melting parameter, the microrotation parameter and thermal conductivity parameter on the velocity, the angular velocity and the temperature profiles in Figures 1-16. The effects of the material parameter K on the velocity profiles $f^{'}$ has been illustrated in Fig. 1. It is seen from this figure that the velocity distribution $f^{'}$ through the boundary layer region increases with the increase of K away from the surface, while the opposite is observed along the sheet. Therefore, according to the same figure, this causes enlargen behavior for the momentum thickness as K increases.

The effect of the material parameter K on the angular velocity profiles h is shown in Figure 2. It is observed that the dimensionless angular velocity decrease as K increase near the surface and the opposite trend is noted away from it. On the other hand with higher values of material parameter K, the values of the angular velocity along the sheet $h(0)$ tends to be more smaller.

Figure 3 represents the effect of material parameter K on the dimensionless temperature profiles $\theta(\eta)$ with heat transfer index. It is evident that within the thermal boundary layer the heating of the fluid layers takes place with an increase in material parameter.

Figure 4 shows the distribution of dimensionless velocity $f'(\eta)$ with different values of slip velocity

© 2022 NSP
Natural Sciences Publishing Cor.

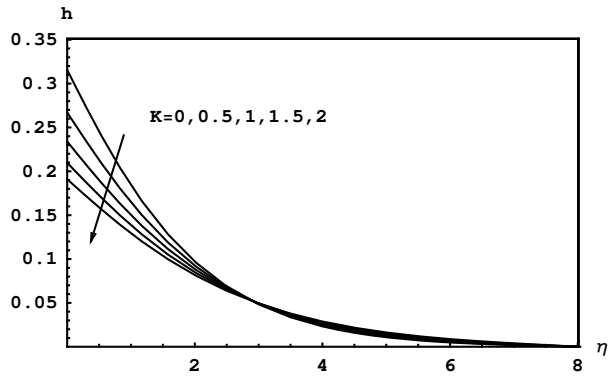

Fig. 2: Angular velocity profiles $h(\eta)$ for different values of K with $\varepsilon = 0.2, M^* = 0.1, \alpha = 0.1, G = 2.0, E_c = 0.5, M = 2.0, P_r = 1.0, m_0 = 0.5$ and $\gamma = 0.2$

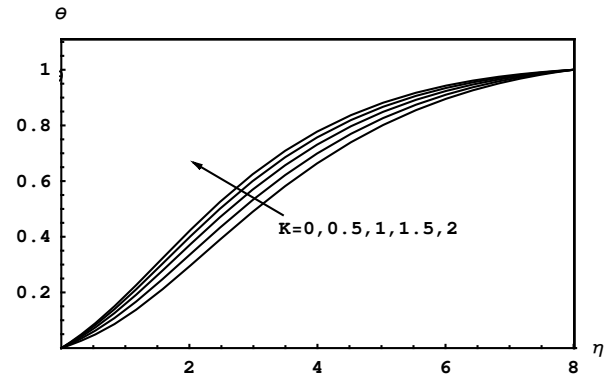

Fig. 3: Temperautre profiles $\theta(\eta)$ for various values of K with $\varepsilon = 0.2, M^* = 0.1, \alpha = 0.1, G = 2.0, E_c = 0.5, M = 2.0, P_r = 1.0, m_0 = 0.5$ and $\gamma = 0.2$

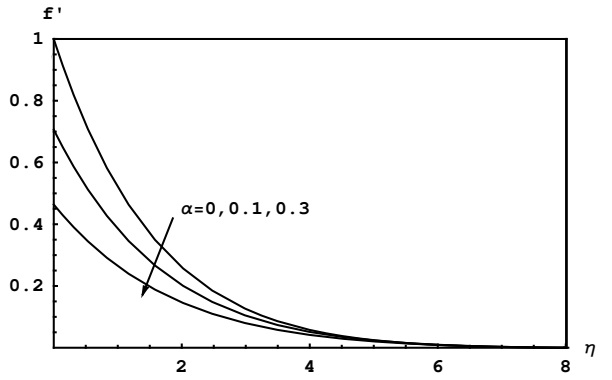

Fig. 4: Velocity profiles $f'(\eta)$ for different values of α with $\varepsilon = 0.2, M^* = 0.1, K = 1.5, G = 2.0, E_c = 0.5, M = 2.0, P_r = 1.0, m_0 = 0.5$ and $\gamma = 0.2$

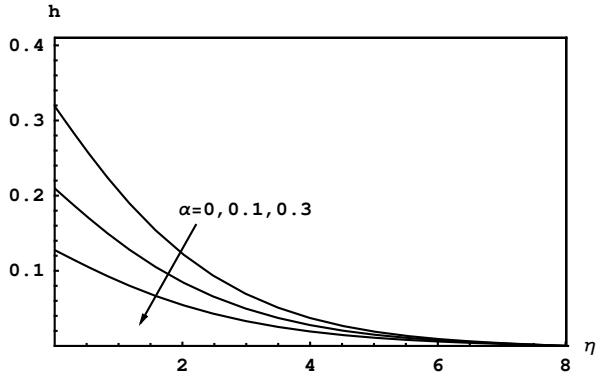

Fig. 5: Angular velocity profiles $h(\eta)$ for different values of α with $\varepsilon = 0.2, M^* = 0.1, K = 1.5, G = 2.0, E_c = 0.5, M = 2.0, P_r = 1.0, m_0 = 0.5$ and $\gamma = 0.2$

parameter α. The graph shows that higher value of α results in smaller velocity distribution throughout the momentum boundary layer. On the other hand with higher values of α, both the boundary layer thickness and the velocity along the sheet $f'(0)$ tends to small behavior.

The effect of the slip velocity parameter α on the dimensionless angular velocity $h(\eta)$ is shown in Figure 5. The higher value of slip velocity parameter of the micropolar fluid exhibits a smaller angular velocity along the sheet $h(0)$. Hence the increase with increasing α.

Fig. 6 illustrates the effects of the slip velocity parameter α on the dimensionless temperature profiles $\theta(\eta)$. It is observed that the temperature distribution $\theta(\eta)$ along the boundary layer decreases with the increase of α.

Fig. 7 shows the variation of velocity profiles for various values of the heat generation parameter $(\gamma > 0)$ and the absorption parameter $(\gamma < 0)$. It is seen that f' decreases with the increase of the heat generation parameter $(\gamma > 0)$ and the absolute value of the heat absorption parameter $(\gamma < 0)$.

The angular velocity profiles for different values of the heat generation parameter $(\gamma > 0)$ and the absorption parameter $(\gamma < 0)$ has been illustrated in Fig. 8, which shows that h increases with the increase of both heat generation parameter $(\gamma > 0)$ and absorption parameter $(\gamma < 0)$ near the surface and the reverse is true at large distance from the surface.

It is noticed that the temperature profiles decrease as ether heat generation parameter $(\gamma > 0)$ or the absolute

© 2022 NSP
Natural Sciences Publishing Cor.

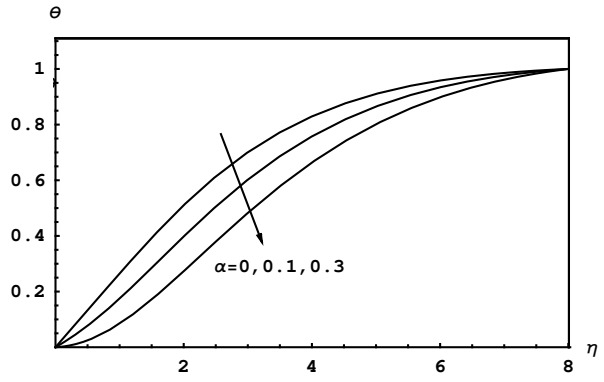

Fig. 6: Temperature profiles $\theta(\eta)$ for different values of α with $\varepsilon = 0.2, M^* = 0.1, K = 1.5, G = 2.0, E_c = 0.5, M = 2.0, P_r = 1.0, m_0 = 0.5$ and $\gamma = 0.2$

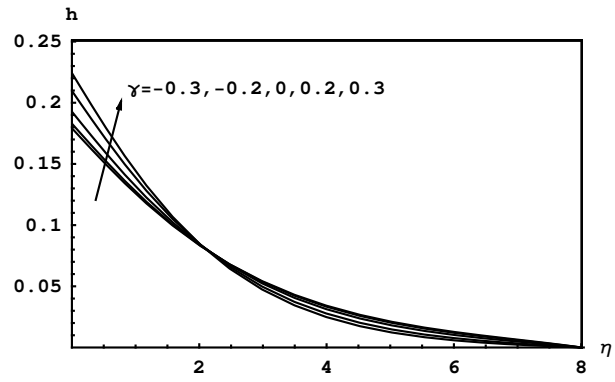

Fig. 8: Angular velocity profiles $h(\eta)$ for different values of γ with $\varepsilon = 0.2, M^* = 0.1, K = 1.5, G = 2.0, E_c = 0.5, M = 2.0, P_r = 1.0, m_0 = 0.5$ and $\alpha = 0.1$

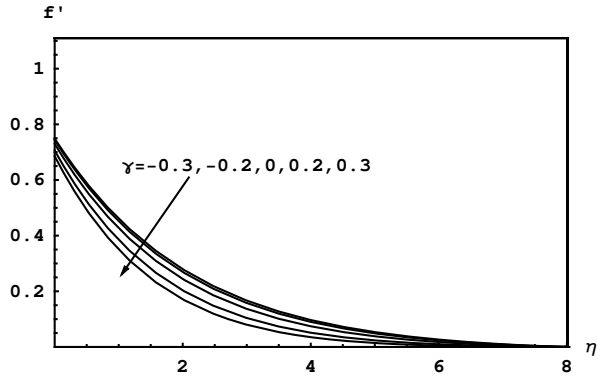

Fig. 7: Velocity profiles $f'(\eta)$ for different values of γ with $\varepsilon = 0.2, M^* = 0.1, K = 1.5, G = 2.0, E_c = 0.5, M = 2.0, P_r = 1.0, m_0 = 0.5$ and $\alpha = 0.1$

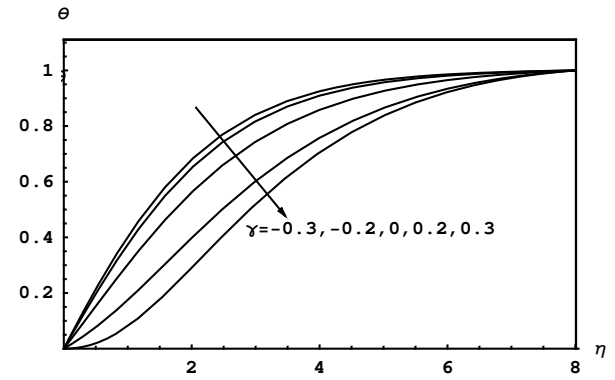

Fig. 9: Temperature profiles $\theta(\eta)$ for different values of γ with $\varepsilon = 0.2, M^* = 0.1, K = 1.5, G = 2.0, E_c = 0.5, M = 2.0, P_r = 1.0, m_0 = 0.5$ and $\alpha = 0.1$

value of the heat absorption parameter ($\gamma < 0$) increase as illustrated in Fig. 9.

The effects of the local Eckret number E_c on the velocity, the angular velocity and the temperature are displayed in Figs. 10, 11 and 12, respectively. Firstly, we must refer here that the viscous dissipation phenomenon means the transformation for some of kinetic energy to an internal energy in the form of induced heat source due to viscous stresses. This impact is foreseeable especially in fluid having large velocity gradients or with highly turbulence levels. It is seen from Fig. 10 that $f^{'}$ increases as the local Eckret number E_c increases.

From Fig. 11 it is shown that h decreases as the local Eckret number E_c increases, while h decreases at large distance from the surface.

Fig. 12 show the effect of the local Eckret number E_c on the temperature profiles θ. It is found that as the local Eckret number E_c increases θ decreases.

It is seen from Fig. 13 that with the increase in the melting parameter M, fluid velocity increases. Hence, the thicker the boundary layer is, the greater the velocity distribution in the momentum boundary layer is.

Fig. 14 presents the effect of the melting parameter M on θ. It is observed that the temperature decreases as M increases. This is in agreement with physical fact that increasing the melting parameter causes higher acceleration to the fluid flow which in turn, increases its motion and causes decreases in the temperature profiles.

The effects of the microrotation parameter G on the angular velocity h illustrated in Fig. 15. From this figure,

© 2022 NSP
Natural Sciences Publishing Cor.

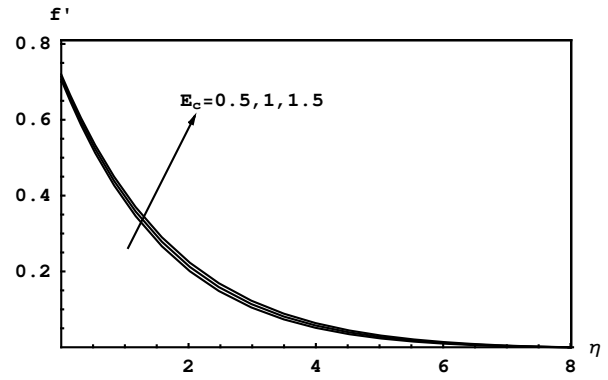

Fig. 10: Velocity profiles $f'(\eta)$ for different values of E_c with $\varepsilon = 0.2, M^* = 0.1, K = 1.5, G = 2.0, \gamma = 0.2, M = 2.0, P_r = 1.0, m_0 = 0.5$ and $\alpha = 0.1$

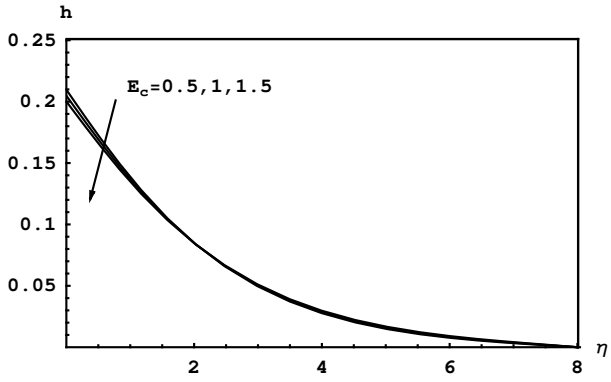

Fig. 11: Angular velocity profiles $h(\eta)$ for different values of E_c with $\varepsilon = 0.2, M^* = 0.1, K = 1.5, G = 2.0, \gamma = 0.2, M = 2.0, P_r = 1.0, m_0 = 0.5$ and $\alpha = 0.1$

it is notice that h increases with the increase of G in an similar way through the boundary layer region.

Fig. 16 displays the effect of thermal conductivity parameter ε. It is observed that the temperature decreases as ε increases. Here, we must refer that the thermal conductivity of a fluid is basically dependent on some factors. These factors include the thermal properties of the fluid, the gradient of the temperature, and the thickness of the boundary layer that the heat follows.

Table 1 illustrates the effects of α, ε, E_c, G, K, M and γ on the local skin-friction coefficient in terms of $f''(0)$, the dimensionless wall couple stress in terms of $h'(0)$ and the local Nusselt number in terms of $-\theta'(0)$. From this Table it is observed that the local skin-friction coefficient, the dimensionless wall couple stress and the local Nusselt number increase with increasing α. Moreover, it is found

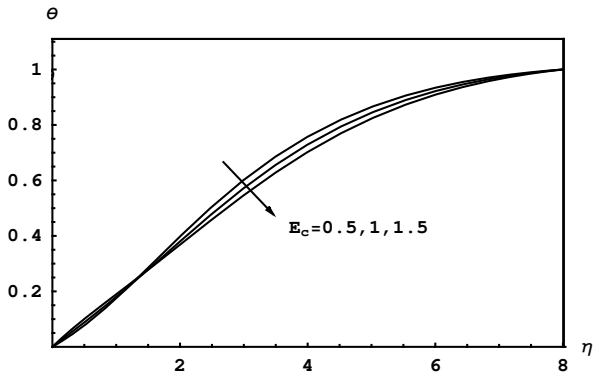

Fig. 12: Temperature profiles $\theta(\eta)$ for different values of E_c with $\varepsilon = 0.2, M^* = 0.1, K = 1.5, G = 2.0, \gamma = 0.2, M = 2.0, P_r = 1.0, m_0 = 0.5$ and $\alpha = 0.1$

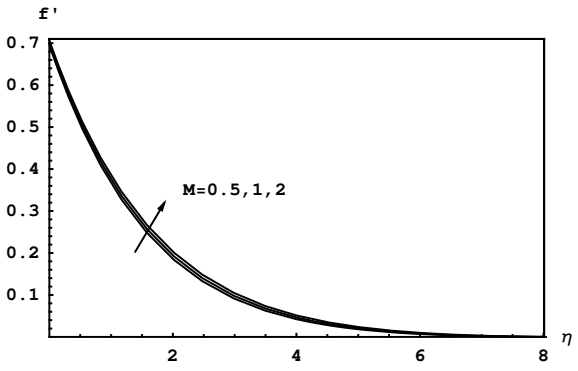

Fig. 13: Velocity profiles $f'(\eta)$ for different values of M with $\varepsilon = 0.2, M^* = 0.1, K = 1.5, G = 2.0, \gamma = 0.2, E_c = 0.5, P_r = 1.0, m_0 = 0.5$ and $\alpha = 0.1$

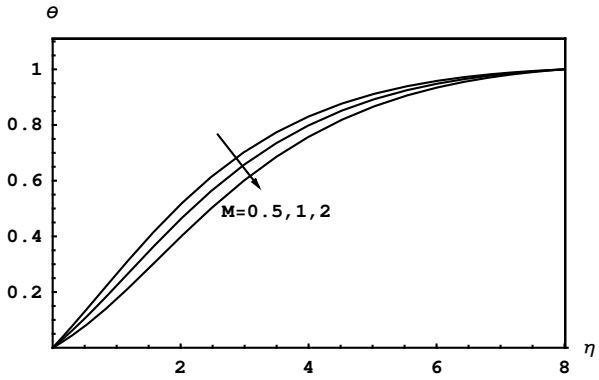

Fig. 14: Temperature profiles $\theta(\eta)$ for different values of M with $\varepsilon = 0.2, M^* = 0.1, K = 1.5, G = 2.0, \gamma = 0.2, E_c = 0.5, P_r = 1.0, m_0 = 0.5$ and $\alpha = 0.1$

© 2022 NSP
Natural Sciences Publishing Cor.

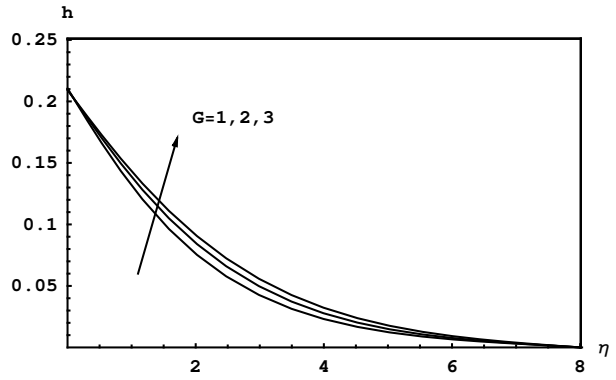

Fig. 15: Angular velocity profiles $h(\eta)$ for different values of G with $\varepsilon = 0.2, M^* = 0.1, K = 1.5, M = 2.0, \gamma = 0.2, E_c = 0.5, P_r = 1.0, m_0 = 0.5$ and $\alpha = 0.1$

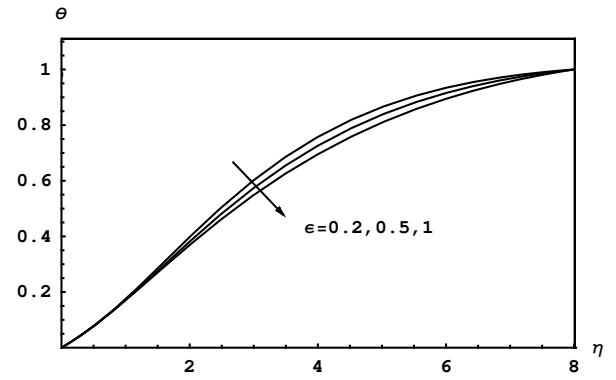

Fig. 16: Temperature profiles $\theta(\eta)$ for different values of ε with $G = 2.0, M^* = 0.1, K = 1.5, M = 2.0, \gamma = 0.2, E_c = 0.5, P_r = 1.0, m_0 = 0.5$ and $\alpha = 0.1$

that, increasing ε leads to a increase in the local skin-friction coefficient and the dimensionless wall couple stress, while the local Nusselt number decreases as ε increases. Also, it is noted that the local skin-friction coefficient and the dimensionless wall couple stress increases as E_c increases , while the local Nusselt number decreases as E_c increases. However, it is shown that the local skin-friction coefficient, the dimensionless wall couple stress and the local Nusselt number increase with increasing G. It is also found that the local skin-friction coefficient and the dimensionless wall couple stress increase with increasing K, but the local Nusselt number decreases as K increases. Also, it is noted that increasing values of M leads to increasing the values of the local skin-friction coefficient, the dimensionless wall couple stress and the local Nusselt number This is because increasing the melting parameter M increases the thermal boundary layer thickness which results in a reduction in temperature gradient at the surface. Finally, we can see that the local skin-friction coefficient, the dimensionless wall couple stress increase with increasing of the heat generation parameter and the heat absorption parameter , while the local Nusselt number decrease with increasing the heat generation parameter and the heat absorption parameter.

5 Conclusions

The problem of the flow of a micropolar fluid with melting heat transfer taking into account the presence of heat generation(absorption) has been investigated. The governing equations of the problem have been transformed into a system of coupled non-linear ordinary differential equations using similarity transformations which is solved numerically by using the Chebyshev spectral method.

Table 1: Values of $f''(0)$, $h'(0)$ and $-\theta'(0)$ with $m_0 = 0.5$, $M^* = 0.1$ and $Pr = 1$

α	ε	E_c	G	K	M	γ	$f''(0)$	$h'(0)$	$-\theta'(0)$
.0	.2	.5	2	1.5	2	.2	-.6383	-.12062	-.2688
.1	.2	.5	2	1.5	2	.2	-.4195	-.07567	-.1331
.3	.2	.5	2	1.5	2	.2	-.2553	-.04376	-.0123
.1	.2	.5	2	1.5	2	.2	-.4195	-.0757	-.1331
.1	.5	.5	2	1.5	2	.2	-.4195	-.0756	-.1332
.1	1	.5	2	1.5	2	.2	-.4182	-.0752	-.1391
.1	.2	.5	2	1.5	2	.2	-.4195	-.0757	-.1331
.1	.2	1	2	1.5	2	.2	-.4097	-.0724	-.1797
.1	.2	2	2	1.5	2	.2	-.4003	-.0693	-.2253
.1	.2	.5	1	1.5	2	.2	-.4211	-.0857	-.1347
.1	.2	.5	2	1.5	2	.2	-.4195	-.0757	-.1331
.1	.2	.5	3	1.5	2	.2	-.4183	-.0695	-.1321
.1	.2	.5	2	0	2	.2	-.6313	-.1445	-.0795
.1	.2	.5	2	.5	2	.2	-.5342	-.1108	-.1016
.1	.2	.5	2	1	2	.2	-.4680	-.0899	-.1195
.1	.2	.5	2	1.5	2	.2	-.4195	-.0757	-.1331
.1	.2	.5	2	2	2	.2	-.3819	-.0653	-.1433
.1	.2	.5	1	1.5	.5	.2	-.4348	-.0809	-.2483
.1	.2	.5	2	1.5	1	.2	-.4274	-.0784	-.1924
.1	.2	.5	3	1.5	2	.2	-.4195	-.0757	-.1331
.1	.2	.5	2	0	2	.3	-.4486	-.0858	-.0008
.1	.2	.5	2	.5	2	.2	-.4195	-.0757	-.1331
.1	.2	.5	2	1	2	0	-.3854	-.0646	-.3004
.1	.2	.5	2	1.5	2	-.2	-.3659	-.0585	-.4044
.1	.2	.5	2	2	2	-.3	-.3584	-.0563	-.4465

The results indicate that the numerical values of the local skin-friction coefficient, the dimensionless wall couple stress and The local Nusselt number increase as the slip parameter, the microrotation parameter and the melting parameter increase. While the local skin-friction coefficient, the dimensionless wall couple stress increase as the thermal conductivity parameter, the Eckret number, the material parameter and the heat generation (absorption) parameter increase. But The local Nusselt number decreases with increasing the thermal conductivity parameter, the Eckret number, the material parameter and the heat generation (absorption) parameter.

© 2022 NSP
Natural Sciences Publishing Cor.

Acknowledgement

The authors would like to thank the reviewers for their valuable comments, which led to the improvement of the work.

Conflict of interest

The authors declare that they have no conflict of interest.

References

[1] Eringen, A. C., Simple microfluids, *International Journal of Engineering Science* 2, 205-217(1964).
[2] Eringen, A. C., Theory of Micropotar Fluids. *J. Math. Mech.* 16, 1-18(1966). .
[3] Eringen, A. C., Theory of thermo-micro fluids. *J. Math. Anal. Appl.* 38, 480-496(1972)..
[4] Ahmadi, G., Self-similar solution of micropolar boundary layer flow over a semi-infinite plate. *Int. J. Engng. Sci.* 14, 639-666(1976)..
[5] Gorla, R. S. R., Micropolar boundary layer flow at a stagnation point on a moving wall. *Int. J. Engng. Sci.* 21, 25-33(1983).
[6] Takher, H. S. and Soundalgekar, V. M., Flow and heat transfer of micropolar fluid past a continuously moving porous plate. *Int. J. Engng. Sci.* 23, 201-205(1985).
[7] Powel, H., *Micropolar fluid model for the brain fluid dynamics.* Int. Conf. Bio-fluid mechanics, UK (1998).
[8] Takhar, H. S., Agarwal, R. S., Bhargava, R. and Jain, S., Mixed convection flow of a micropolar fluid over a stretching sheet. *Heat and Mass Transfer* 34, 213-219(1998).
[9] Bhargava, R., Kumar, L. and Takhar, H.S., Mixed convection from a continuous surface in a parallel moving stream of a micropolar fluid. *Heat and Mass Transfer* 39, 407-413 (2003).
[10] Nazar, R., Amin, N. and Pop, I., Stagnation point flow of a micropolar fluid towards a stretching sheet. *Int. J. Non-Linear Mech.* 39, 1227-1235 (2004).
[11] Hayat, T., Abbas, Z. and Javed, T., Mixed convection flow of a micropolar fluid over a non-linearly stretching sheet. *Phys. Lett. A* 372, 637-647(2008).
[12] Lok, Y. Y., Pop, I., Chamkha, A. J., Non-orthogonal stagnation-point flow of a micropolar fluid. *Int. J. Eng. Sci.* 45, 173-184 (2007).
[13] Ishak, A., Thermal boundary layer flow over a stretching sheet in a micropolar fluid with radiation effect. *Meccanica* 45, 367-373(2010).
[14] Mahmoud, M. A. A. and Waheed, S. E., MHD stagnation point flow of a micropolar fluid towards a moving surface with radiation. *Meccanica* 47, 1119-1130(2012).
[15] Slayi, S. A., Idriss, H. F. and Ashmawy, E. A., Time dependent slip flow of a micropolar fluid between two parallel plates through state space approach. *Global Journal of Pure and Applied Mathematics* 12, 1709-1722(2016).
[16] Mabood F., Abdel-Rahman R. G. and Lorenzini G.,Effect of Melting Heat Transfer and Thermal Radiation on Casson Fluid Flow in Porous Medium over Moving Surface with Magnetohydrodynamics. *Journal of Engineering Thermophysics* 25,536-547 (2016).
[17] Anuradha S. and Punithavalli R. MHD Boundary Layer Flow of a Steady Micro polar Fluid along a Stretching Sheet with Binary Chemical Reaction.*International Journal of Applied Engineering Research* 14, 440-446 (2019).
[18] P. Somasekhara Reddy and D.R.V. Prasada Rao, Influence of Soret and Dufour Effects on Unsteady Hydromagnetic Heat and Mass Transfer Flow of a Micropolar Fluid past a Stretching Sheet with Heat Sources. *International Journal of Scientific and Innovative Mathematical Research*, 6, 1-14(2018).
[19] Jena S. K., Mathur M. N., Similarity solution for laminar free convection flow of thermo-micropolar fluid past a non-isothermal vertical flat plate. *Int. J. Eng. Sci.*, 19, 1431-1439 (1981).
[20] Peddieson, J., McNitt, R. P., Boundary-layer theory for a micropolar fluid. *Recent Adv. Eng. Sci.* 5, 405-426 (1970).
[21] Epstein M. and Cho D. H., Melting heat transfer in steady laminar flow over a flat plate. *ASME J. Heat Transfer* 98, 531-533 (1976).
[22] Bachok N., Ishak A. and Pop I., Melting heat transfer in boundary layer stagnation-point flow towards a stretching/shrinking sheet. *Physics Letters A* 374, 4075-4079 (2010).
[23] El-Gendi S. E., Chebyshev solution of differential, integral and integro-differential equations. *Computer J.* 12, 282-287 (1969).

Shimaa E. Waheed received the PhD degree in Applied Mathematics at Banha University. Here research interests are in the areas of applied mathematics and mathematical physics including numerical methods for non linear ordinary differntial equations. She has published research articles in reputed international journals of mathematical and engineering sciences.

Ahmed M. Megahed is Associate Professor of Mathematical at Banha University. His research interests are in the areas of applied mathematics and mathematical physics including numerical methods for non linear ordinary differntial equations. He has published research articles in reputed international journals of mathematical and engineering sciences.

© 2022 NSP
Natural Sciences Publishing Cor.